Article

Vimentin Enhances Cell Elastic Behavior and Protects against Compressive Stress

M. G. Mendez, D. Restle, and P. A. Janmey*
Institute for Medicine and Engineering, University of Pennsylvania, Philadelphia, Pennsylvania

ABSTRACT Vimentin intermediate filament expression is a hallmark of epithelial-to-mesenchymal transitions, and vimentin is involved in the maintenance of cell mechanical properties, cell motility, adhesion, and other signaling pathways. A common feature of vimentin-expressing cells is their routine exposure to mechanical stress. Intermediate filaments are unique among cytoskeletal polymers in resisting large deformations in vitro, yet vimentin's mechanical role in the cell is not clearly understood. We use atomic force microscopy to compare the viscoelastic properties of normal and vimentin-null ($vim^{-/-}$) mouse embryo fibroblasts (mEFs) on substrates of different stiffnesses, spread to different areas, and subjected to different compression patterns. In minimally perturbed mEF, vimentin contributes little to the elastic modulus at any indentation depth in cells spread to average areas. On a hard substrate however, the elastic moduli of maximally spread mEFs are greater than those of $vim^{-/-}$mEF. Comparison of the plastic deformation resulting from controlled compression of the cell cortex shows that vimentin's enhancement of elastic behavior increases with substrate stiffness. The elastic moduli of normal mEFs are more stable over time than those of $vim^{-/-}$mEFs when cells are subject to ongoing oscillatory compression, particularly on a soft substrate. In contrast, increasing compressive strain over time shows a greater role for vimentin on a hard substrate. Under both conditions, $vim^{-/-}$mEFs exhibit more variable responses, indicating a loss of regulation. Finally, normal mEFs are more contractile in three-dimensional collagen gels when seeded at low density, when cell-matrix contacts dominate, whereas contractility of $vim^{-/-}$mEF is greater at higher densities when cell-cell contacts are abundant. Addition of fibronectin to gel constructs equalizes the contractility of the two cell types. These results show that the Young's moduli of normal and $vim^{-/-}$mEFs are substrate stiffness dependent even when the spread area is similar, and that vimentin protects against compressive stress and preserves mechanical integrity by enhancing cell elastic behavior.

INTRODUCTION

Vimentin is a type III intermediate filament (IF) protein initially expressed during the primary epithelial to mesenchymal transition (EMT) by mesodermal cells as they adopt the motility that accompanies gastrulation, and expression continues into adulthood for mesenchymal cell types (1). This developmental regulation has led to vimentin's widespread use as a marker of EMT and mesenchymal cells. Vimentin is transiently expressed in some nonmesenchymal cell types during development, and may be reexpressed in adulthood following injury, e.g., by microglia (2). Vimentin expression also accompanies the progression of diseases including carcinoma (3) and fibrosis (1).

It is common for mesenchymal cells, including fibroblasts, endothelial cells, and multipotent stromal cells, to be routinely subject to force. The pulling, pushing, and frictional forces that accompany cell motility (4), or the shear forces generated by blood (5) or airway surface fluid flow (6) are examples of forces that directly impact mesenchymal cell types. In general, disease processes accompanied by increased vimentin expression are also accompanied by disease-relevant cell mechanical changes, e.g., the onset of motility by previously nonmotile metastatic cells or the stiffening of a fibrotic tissue (7,8).

In vitro, in silico, and cell-based results show that vimentin is involved in the establishment or maintenance of cell and tissue mechanical properties, and evidence obtained from studies of other IF types confirms that this is a common property of IF. Vimentin polymer networks in solution increase their shear elastic modulus at least 30-fold in response to strain, with no accompanying loss of elasticity at strains up to more than 100%, which starkly contrasts the more brittle actin and tubulin-based networks that rupture under significantly less strain (9). The cytoplasm of normal fibroblasts is twice as stiff as that of comparable vimentin-null fibroblasts when measured by displacement of internalized particles (10). Vimentin loss also renders fibroblasts more easily deformable (11), and chondrocytes (12) and lymphocytes (13) soften when vimentin networks are reorganized away from the cell periphery or pharmacologically disrupted, respectively. Vimentin loss or disruption also reduces the cells' compressibility in response to applied strain (14). Modeling studies support a role for vimentin in the cells' resistance to tensile strain (15). Together, vimentin's strain-stiffening behavior, durability relative to microfilaments and microtubules, and contribution to compressibility, as well as the remodeling of the vimentin network associated

Submitted January 15, 2014, and accepted for publication April 30, 2014.
*Correspondence: janmey@mail.med.upenn.edu
Editor: David Piston

0006-3495/14/07/0314/10 $2.00
http://dx.doi.org/10.1016/j.bpj.2014.04.050

with cell softening, show that vimentin stiffens cells and indicate that it is especially protective against large strains. Studies showing mechanical functions for other IF types further highlight the mechanical functions of IF proteins: Mutant keratins render keratinocytes less able to withstand deformation (16) and keratinocytes devoid of all keratins are softer and deform more easily than cells with low keratin expression levels (17); desmin mutations can either increase or decrease the stiffness of cells containing heteropolymeric desmin/vimentin networks (18); and the loss or mutation of lamin A/C perturbs nuclear stiffness (19,20).

To clarify how vimentin contributes to the determination and/or maintenance of cell mechanical properties, we compare the viscoelastic properties of normal and vim$^{-/-}$ mEF grown on hard and soft substrates. Normal vimentin-containing mEFs are stiffer than vim$^{-/-}$ mEFs when cells are maximally spread. Vimentin loss reduces cell elasticity and increases the overall variability of cell mechanical properties. These effects vary with substrate elastic modulus and alter in response to ongoing or increasing compressive stress. These results show that vimentin modulates cell viscoelastic behavior and protects against mechanical stress.

METHODS

Cell culture

Mouse embryo fibroblasts (mEFs) and vimentin-null mEF (vim$^{-/-}$ mEF) were kindly provided by J. Ericsson (Åbo Akademi University, Turku, Finland) and maintained in DMEM including HEPES and sodium pyruvate (Life Technologies; Grand Island, NY) supplemented with 10% fetal calf serum and nonessential amino acids (Life Technologies). Cells were maintained in log-phase growth and subcultured 24 h before all experiments. Cells were seeded at low densities before atomic force microscopy (AFM) to minimize cell-cell contact while maintaining cell vitality.

Cell spreading

Glass coverslips coated with 100 μg/ml collagen I (BD Biosciences, Franklin Lakes, NJ) or fibronectin (isolated from human plasma) were equilibrated in mEF medium in a tissue culture incubator before placement in a Tokai-Hit Imaging Chamber (Tokai Hit, Shizuoka-ken, Japan) that maintained a humid, 37°, 5% CO_2 environment. Using imperfections on the gel surface, iVision (BioVision Technologies, Exton, PA) was used to focus a Leica DMIRE2 (Leica, Buffalo Grove, IL) equipped with an ASI x/y/z stage (BioVision Technologies) and Hamamatsu Camera (Hamamatsu, Japan) at multiple fields of view. Cells were trypsinized, seeded onto the gel, and images subsequently captured every minute. Spreading data were obtained by tracing cell peripheries at each time point using ImageJ (Image J Software; NIH, Bethesda, MD). Cells were excluded if they migrated out of the field of view or contacted another cell.

Two-dimensional substrate preparation

Polyacrylamide (PAA) substrates were prepared as described (21), using 150 μl of gel mixture to form each 22 mm^2 gel: 6 kPa, 7.5% PAA w/v +106 μl 2% bis-acrylamide (BioRad, Hercules, CA); 36 kPa, 12% PAA +196 μl 2% bis-polyacrylamide. Gels were activated by Sulfo-SANPAH (Thermo Scientific; Waltham, MA) crosslinking followed by incubation in 100 μg/ml fibronectin, as described (21,22).

AFM

For all experiments, data were collected from single (not in contact with any other cell), interphase cells using a Bruker BioScope BS-3 (Bruker; Santa Barbara, CA) making either single or periodic indentations at 2.0 Hz. Probes consisted of a 3.5 μm glass bead glued (Norland Optical Adhesive 63) along the centerline within 500 nm of the leading edge of a tipless cantilever (NP-O10; Bruker) of 0.06 N/m nominal stiffness. The spring constant of each tip was determined before use by the thermal tune method (23).

Determination of contact points and Young's moduli were made as previously described using custom-written MATLAB software (The MathWorks, Natick, MA) (24,25). Briefly, indentations were sampled at a rate of 128 points over a 3 μm ramp. The point at which the cantilever tip made contact with each cell (contact point) was determined by identifying the first deviation from the straight-line portion of the force versus displacement curve (GraphPad Prism 5; GraphPad Software; La Jolla, CA). Indentations were made to approximate depths at the time of indentation, and then actual depths determined by subtracting the distance from the contact point to the deepest point, less the cantilever deflection from the total distance traveled by the piezo (3 μm). Data were fit with the Hertz model as previously described to determine Young's modulus (24). Poisson's ratio is assumed to be 0.5 (26). Depth-dependent moduli are calculated by curve-fitting from the contact to the deepest point. For experiments over time, the cantilever oscillated at 2 Hz over a 3 μm ramp in a consistent position relative to the substrate, such that the initial portion of the descent was not in contact with the cell and cells were indented 500–1000 nm.

Plasticity index

The areas under the extension and retraction curves were found by identifying the contact and loss-of-contact points, respectively (GraphPad Prism) from ASCII files of the data points generated by the BioScope BS-3. These data were used to calculate the PI metric [PI = 1-($Area_{Extension}$/$Area_{Retraction}$)] (27).

Three-dimensional (3D) gel preparation and contraction assay

3D collagen gels were prepared by resuspending counted and pelleted cells to achieve final concentrations of 1× DMEM (from 5×; Life Technologies), 10% fetal calf serum, and 2 mg/ml collagen I in 3 mL final volume, cultured in a 35 mm dish. For some experiments, 0.1% fibronectin was added and collagen concentration reduced to 1.9%. For contraction assays, gels were plated on day (0), freed from the sides of the dish by running a pipette tip around the circumference on day (1), and then photographed every 24 h until day (7), at which time they were Hoechst-stained and imaged to count cells. Collagen gel shear moduli were determined on day (1) and (7) using a TA Instruments (New Castle, DE) RFS II equipped with an 8 mm parallel plate coated with double-sided tape (Scotch 3M; St. Paul, MN). Gels were maintained at 37° and enclosed in a humidified chamber. Three regions of each gel were measured at 2 rad/s and the averaged result counted as one experiment.

Statistics

Statistical significance is determined using the nonparametric Mann-Whitney test with two tails at the 95% confidence interval (GraphPad Prism), and p-values <0.05 are considered significant. The results of experiments are presented as $\pm$ SE or $\pm$ SD as appropriate, using the number of experiments as n except where stated otherwise.

RESULTS

Effect of vimentin loss on cell spreading is substrate dependent

We began by determining the range of substrate stiffnesses on which normal and vim$^{-/-}$ mEFs attach and spread. On fibronectin-coated PAA, consistent with studies conducted using a variety of other cell types (22,28), the spread areas of both cell types increase with increasing substrate elastic modulus (Fig. 1 *A*). Cells containing vimentin spread more on softer substrates (750 Pa and 6 kPa), whereas vim$^{-/-}$ mEFs spread more on tissue culture plastic (TCplas).

To facilitate comparisons of cells' mechanical properties, 6 kPa was selected as the soft substrate, as this was the softest PAA on which a significant proportion of mEFs would spread and elongate, similar to how mEFs grow on hard substrates such as glass or TCplas (Fig. 1, *B* and *D*). On softer substrates, cells were significantly rounder and tended to roll away from the cantilever tip when indented. Because of possible interdependencies among substrate stiffness, cell spread area and cell stiffness are not yet clearly understood, two populations of cells were selected for further study. For most experiments, cells with adherent areas of 2500–4000 μm^2 were selected (Fig. 1, *B* and *C*; *curly brackets*). In addition to similar spread areas, cells selected for AFM had exactly two protrusions extending in opposite directions from a centrally positioned nucleus (Fig. 1, *D–F*). Because vimentin is enriched in the endoplasmic region (29) and long vimentin filaments do not extend into lamellipodia in fibroblasts (30), AFM measurements were performed within the endoplasmic region. To investigate the relationship between mechanical properties and spread area, a second population of cells was selected for AFM consisting of cells spread to $\geq$14,000 μm^2 (Fig. 1 *C*, *square bracket*). For these experiments cells were chosen because of a large spread area irrespective of other morphological characteristics, and also indented in the endoplasmic region.

In addition to examining the spread areas of the two cell types after 24 h, normal and vim$^{-/-}$ mEFs were examined for differences in their spreading rates immediately following trypsinization and replating. Cells were allowed to spread on fibronectin (Fn)- or collagen I (colI)-treated TCplas. Normal and vim$^{-/-}$ mEFs spread more rapidly on the Fn-coated substrate (Fig. 1 *G*). On both substrates, the two cells types began spreading at similar rates but

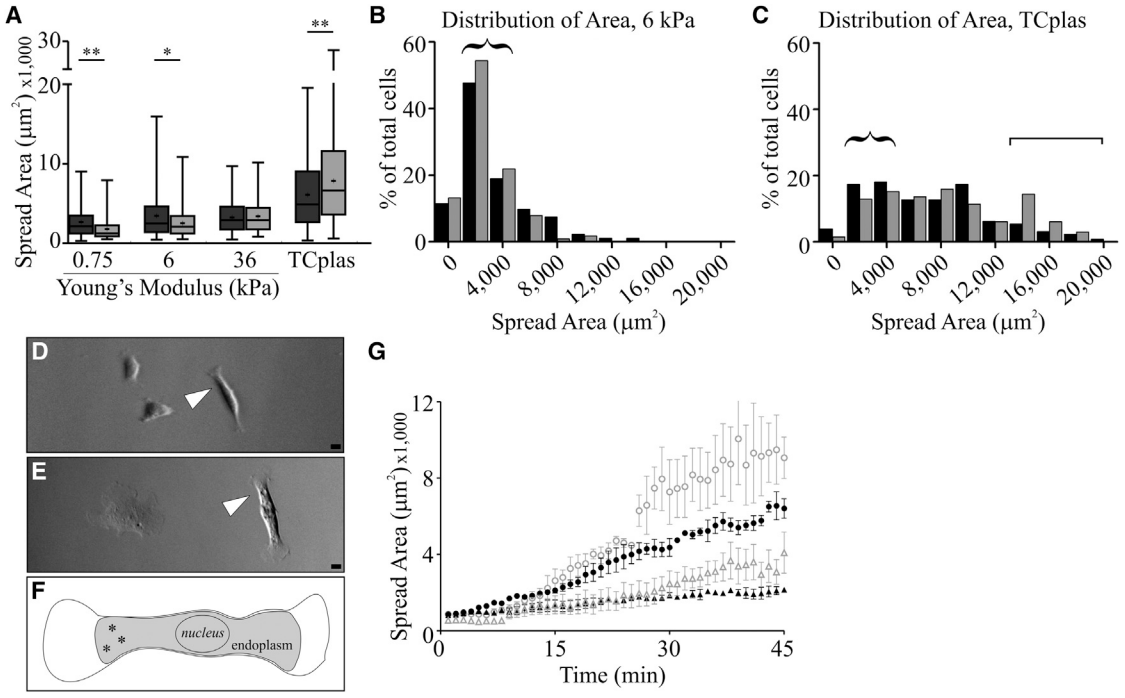

FIGURE 1 Cell spread area of normal and Vim$^{-/-}$ mEFs. Normal mEF spread more than vim$^{-/-}$ on soft substrates, but less on TCplas (*A*; *dark bars*, mEF; *lighter bars*, vim$^{-/-}$ mEF; 750 Pa: mEF, 2686 $\pm$ 2203 vs. vim$^{-/-}$, 1806 $\pm$ 1350, $p < 0.05$; 6 kPa: mEF, 3457 $\pm$ 2870 vs. vim$^{-/-}$, 2555 $\pm$ 1811, $p < 0.02$; TCplas: mEF, 6120 $\pm$ 4272 vs. vim$^{-/-}$, 7878 $\pm$ 5441, $p < 0.05$; all $n > 100$ cells; errors are SD). Frequency distributions of cell spread areas on 6 kPa PAA (*B*) and TCplas (*C*; *black*, mEF; *gray*, vim$^{-/-}$ mEF) show the availability of cells with spread areas ~2500–4000 μm^2 on both substrates (*curly brackets*; $n = 3$, $\geq$50 cells per experiment) and cells with areas >14,000 μm^2 on TCplas (*square bracket*). Differential interference contrast images of exemplar cells (indicated by *arrowheads*) on 6 kPa PAA (*D*) and TCplas (*E*) show the bipolar shapes of 2500–4000 μm^2 cells selected for AFM, also illustrated in (*F*; asterisks indicate location of AFM indentation in the distal endoplasmic region). Bars = 20 μm. Cell spread areas were determined following subculturing beginning from the first frame after which the cell stopped translocating, indicating attachment to the substrate (*G*; *solid shapes*, mEF; *open*, vim$^{-/-}$; Fn-TCplas, *circles*; ColI-TCplas, *triangles*). ~26 min postattachment, vim$^{-/-}$ mEFs begin to spread more rapidly than normal mEFs on Fn- or Col1-treated TCplas ($n = 8$ cells per condition collected over a minimum of 2 experiments; errors SE).

after ~26 min vim$^{-/-}$ mEFs accelerate their spreading rate relative to normal mEF. On Fn, the initial extent of spreading (first 45 min) of the vim$^{-/-}$ mEF exceeded the cell spread area evident after 24 h (cf. Fig. 1, *G* to *A*).

Vimentin increases cell stiffness

To determine vimentin's contribution to Young's modulus, sparsely seeded cells were indented by AFM 24 h after subculturing. Each cell was indented 3–5 times by a single cantilever incursion, with indentations spaced at least a few μm apart. Next, the precise indentation depth and Young's modulus, E, were determined for each indentation. Data were binned by 100–200 nm indentation depth increments, and averaged by depth and E. Three groups of cells were measured: cells with spread areas between 2500–4000 μm^2 on 6 kPa PAA and TCplas, and cells spread to more than 14,000 μm^2 on TCplas.

To determine whether normal and vim$^{-/-}$ mEFs exhibit differences in E, data were analyzed two ways. To facilitate comparisons to previous studies, stiffness profiles over the entire depth of the regions tested were compared by fitting unbinned data with single exponential curves. In less spread cells (Fig. 2, *A* and *B*; *insets*) these curves fall within the 95% confidence intervals of one another, indicating no significant difference between cell types. To determine whether curve-fitting might obscure differences within specific regimes, the same data were binned, averaged, and compared by depth. Significant differences are not detectable by AFM in the Young's moduli of normal versus vim$^{-/-}$ mEF spread between 2500–4000 μm^2 on a soft substrate (Fig. 2 *A*) by either analysis. Nor is there a difference in cells similarly spread on a hard substrate (Fig. 2 *B*). Both cell types, however, are stiffer on TCplas than on 6 kPa PAA.

To determine whether vimentin contributes to possible spreading-associated stiffening, we measured the Young's moduli of well-spread cells on TCplas (Fig. 1 *C*). On TCplas, normal and vim$^{-/-}$ mEF stiffness correlate with spreading, and normal mEF stiffen more than vim$^{-/-}$ relative to less spread cells (Fig. 2 *C*).

Vimentin decreases cell plasticity in a substrate-dependent manner

When AFM indentation is used to determine elastic modulus, data collected from the descending (loading) stroke of the cantilever are evaluated (see Methods), but the ascending (unloading) stroke is generally not taken into account. Comparing the force versus displacement (F vs. D) curves generated by the two strokes, however, is informative as to the elastic and viscous components of the modulus. We use the plasticity index (PI) metric to quantify the hysteresis between the two strokes to determine whether vimentin modulates cell viscoelastic properties (Fig. 3 *A*; (27)).

On PAA substrates, both cell types dissipate more of the work done during AFM indentations than on TCplas (Fig. 3 *B*, 6 and 36 kPa versus TCplas). The PI of normal mEF differs across each substrate condition tested, indicating that PI reflects a property modulated by substrate stiffness. The PI of vim$^{-/-}$ mEFs however, are more broadly distributed, do not differ across PAA conditions, and reflect a less viscous response when cells are grown on TCplas. Furthermore, only on TCplas does the PI differ between the two cell types.

Vimentin helps cells withstand repetitive stress on hard and soft substrates

The preceding AFM experiments were performed on naive cells. By perturbing each cell only enough to perform the indentation, we assayed the resting state accompanied by the minimum possible biochemical or rheological response. In contrast, indenting cells repeatedly over time is useful in

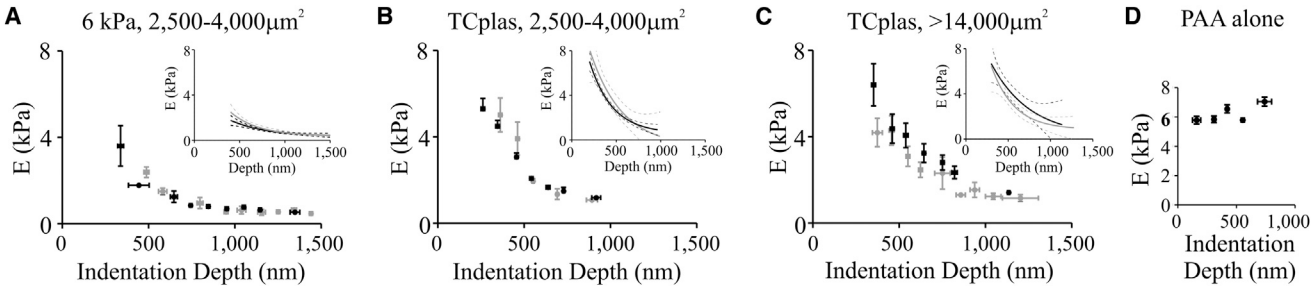

FIGURE 2 Vimentin loss decreases internal cell elastic modulus. AFM indentation of normal (*black*) or vim$^{-/-}$ mEF (*gray*) spread to 2,500–4,000 μm^2 on 6 kPa PAA (*A*; average E at 600 nm; 6 kPa, mEF 1,253 ± 589 Pa, $n = 67$ and vim$^{-/-}$ 1494 ± 374, $n = 53$) or TCplas (*B*; TCplas; mEF 1833 ± 329, $n = 58$ and vim$^{-/-}$ 1959 ± 209, $n = 45$; $p < 0.05$; error = SD; min 3 experiments) show no difference in the Young's moduli of the two cell types on either substrate, but a significant difference between either cell type on the soft compared to the stiff substrate. Insets show curve fits (*solid lines*) and 95% confidence intervals (*dashed lines*) for the same data, unbinned. Unlike less-spread cells, maximally spread normal mEFs are stiffer than vim$^{-/-}$ mEFs (*C*; average E at 600 nm; mEF 3512 ± 1479 Pa and vim$^{-/-}$ 2855 ± 1287, $p < 0.02$; $n = 46$; error = SD). Furthermore, both cell types are stiffer when maximally spread than when less spread on TCplas. As a control, 6 kPa PAA gels were indented in regions devoid of cells (*D*; $n = 30$; error = SD).

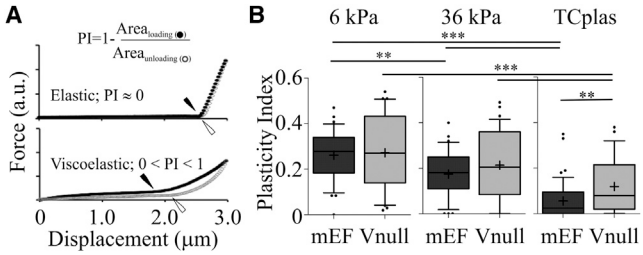

FIGURE 3 Vimentin loss increases cell viscosity on a hard substrate. The PI metric (*A*, *top*) of a perfectly elastic material is 0, and PI increases to 1.0 as the viscous component, and therefore the hysteresis between the force exerted by the cell on the descending and ascending cantilever tip, increases. Areas are determined under the F versus D curves generated by the descending (*loading*; *black*) cantilever from the contact point (indicated by *black arrowheads*) to the deepest point, and under the ascending (*unloading*; *gray*) strokes from the deepest point to the loss-of-contact point (*open arrowheads*). On all substrates, the PI of vim$^{-/-}$ cells (*lighter bars*) are more broadly distributed than those of normal mEFs (*darker bars*; *B*; *whiskers* show 10–90 percentile values; + indicate means). The PI of normal mEFs differ across all conditions tested (*** indicates $p < 0.0001$; ** indicates $p < 0.002$); the PI of vim$^{-/-}$ mEFs are greater on PAA versus TCplas; only on the stiffest substrate do the PI of normal and null mEFs differ from one another. These results were generated by analysis of the same force versus deflection curves presented in Fig. 2.

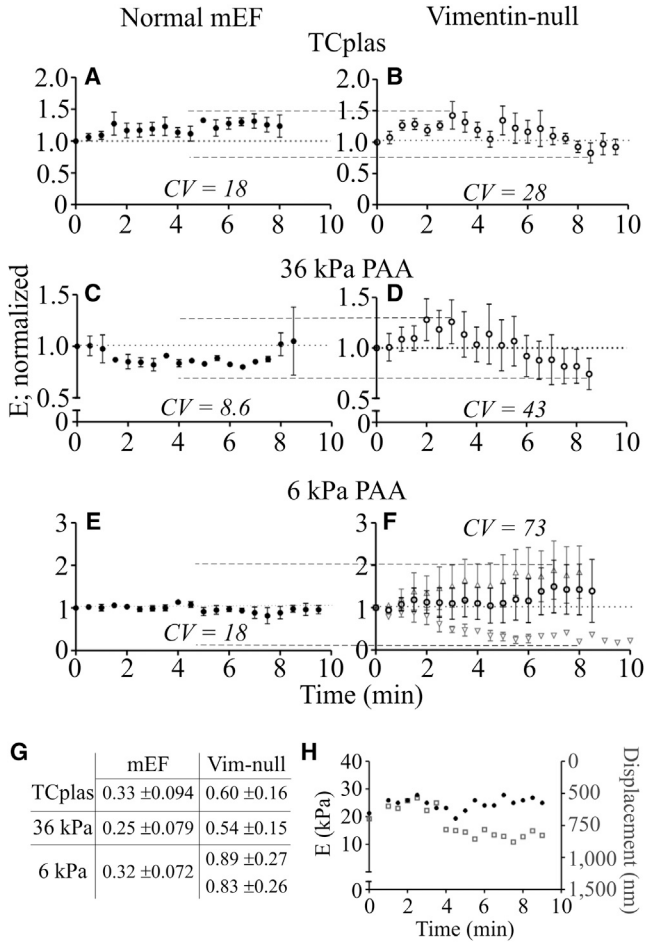

FIGURE 4 Vimentin modulates the changes in elastic modulus that accompany repetitive stress. Cells were indented constantly at 2 Hz. Every 30 s (i.e., every 59th) F versus D curve was retained for evaluation and the resulting E averaged by time point. On all substrates, the E of normal mEF (*solid circles*; *A*, *C*, and *E*) vary less over time than those of vim$^{-/-}$ cells on the same substrate (*open circles*; *B*, *D*, and *F*). Coefficients of variance (CV) are shown for each condition; dashed lines (*A*–*F*) indicate SD (*G*; mean ± SD; 8 cells per condition). Note the manyfold increase in variability in the vim$^{-/-}$ mEFs. No correlation was observed between stiffness changes and cell height, as illustrated by a representative cell in which stiffness (*H*; *black circles*) remains relatively constant, although height (*gray squares*; determined by intrusion depth) changes more dramatically.

determining the extent of vimentin's contribution to the maintenance of mechanical properties. For subsequent experiments, cells were indented constantly at 2 Hz and a F versus D curve retained for analysis every 30 s, from which the Young's modulus and cell height were determined.

On all substrates tested, vimentin minimizes the magnitude of changes in E, as well as the intercell variability (Fig. 4). The smaller deviations in E over the course of the experiment by the normal mEFs (Fig. 4, *A*, *C*, *E*, and *G*), show that vimentin protects against the mechanical stress of repetitive compression. The greater intercell variability and time point-to-time point fluctuations in the E of the vim$^{-/-}$ cells (*B*, *D*, *F*, and *G*) support this conclusion by showing a general reduction in the regulation of cell stiffness. This is most apparent in the vim$^{-/-}$ cells on the softest substrate (Fig. 4 *F*), which exhibited a biphasic response in which some cells softened, whereas others stiffened, varying in E by ~100% in either direction. This dual response was not evident under other conditions.

To determine whether changes in the heights of the cells caused the changes in Young's modulus, data were analyzed for correlations between changes in the contact point and the elastic modulus over time. No consistent relationship was observed between cell height and the magnitude or direction of changes in E (Fig. 4 *H*). In control experiments performed on nonseeded areas of TCplas or PAA substrates, the point at which the cantilever made contact with the substrate did not change over time, supporting the conclusion that the differences in intrusion depths reflect changes in cell height rather than changes in the path of travel of the cantilever.

Vimentin protects against increasing compression

In vivo, cells' protective mechanisms against normal recurring stresses often differ from mechanisms that may exist to protect against potentially damaging abnormal worsening stress; increases in the magnitude of a stress may trigger different responses than a similar type of stress applied at a constant or repetitive level. To determine whether vimentin plays a role in the protection against increasing compressive stress, normal and vim$^{-/-}$ mEFs were indented constantly at 2 Hz as above (Fig. 4), with the added parameter of dropping the cantilever in 300 nm increments at 30 s intervals. Indentation depths were then determined for each

cantilever position, and the data binned by indentation depth to examine the properties of the different regions within the cells relative to the distance from the cell surface.

When growing on a soft substrate, normal mEF stiffen more in response to subsequently deeper indentations than vim$^{-/-}$ mEF (Fig. 5 *A*). Cells growing on TCplas respond in the opposite fashion, with normal mEF stiffening slightly and vim$^{-/-}$ cells significantly more so (Fig. 5 *B*). Both sets of responses, however, indicate a strikingly different internal environment than the softening with depth observed when the cantilever intrudes only once onto a cell at any location (Fig. 2). Control indentations of unseeded regions of PAA showed no stiffness change with depth, as expected for linearly elastic PAA (Fig. 5 *C*; (22)). Average *F* versus *D* curves of cells on TCplas show that the two cell types respond similarly in the most apical regions (Fig. 5, *D* and *E*), and that differences become apparent with increasing intrusion. Of note, the vim$^{-/-}$ cells did not flow away from the intruding tip; there were no obvious changes in spread area or consistent differences in cell height following indentation. These results, considered in light of the results of indentations made at the same rate but to the same depth (Fig. 4), indicate that vimentin's role is enhanced when the rate or magnitude of compression is variable, and suggest that the vimentin network may provide significant resistance against large or unusual stresses.

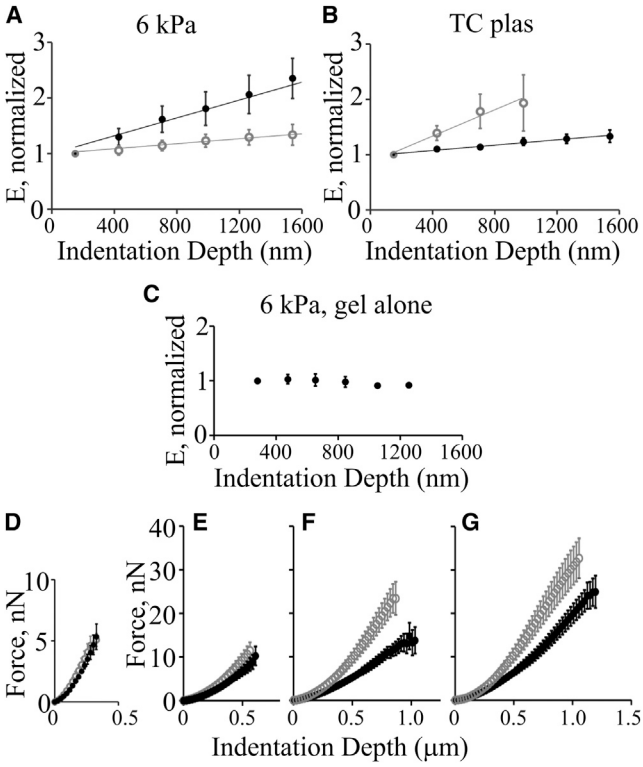

FIGURE 5 Vimentin's role in the protection against increasing compression varies with substrate stiffness. mEF (*black*) and vim$^{-/-}$ mEF (*gray*) were indented constantly at 2 Hz accompanied by a series of 300 nm decreases in cantilever height at 30 s intervals. F versus D curves were obtained rapidly after each cantilever height adjustment. Stiffness values were computed, normalized to the initial value obtained for each cell, and averaged. On 6 kPa PAA, vim$^{-/-}$ mEF stiffen by 33% ± 43% and mEF by 133% ± 88% over the course of 3 min and 6 increases in indentation depth (*A*; $n = 9$, $p < 0.0001$). In contrast, cells on TCplas respond in the opposite fashion (normalized E of mEF increases 33% ± 36% vs. vim$^{-/-}$ (B), 90% ±120%, $n = 8$, $p < 0.001$, errors SD). Control indentations of unseeded regions of PAA show no stiffness change with depth (*C*; $n = 8$). Nonnormalized values representing the same data show no difference in the F versus D profiles of the two cell types for the first (*most apical*) indentation (*D*; 300–500 nm indentation depth). After 30 s and the next deeper indentation, F versus D curves are still similar (*E*; 600–800 nm). Ongoing compression and subsequently deeper indentations reveal differences in the responses of the two cell types in the 800–1100 nm (*F*) and 1100–1300 nm (*G*) ranges.

Vimentin's effect on contractility is substrate and cell density dependent

Because of the relationships among cell stiffness, tension-generating ability, and contractility, we performed collagen contraction assays to examine vimentin's role in the cells' tension generation. 24 h after polymerization or maintained alongside cells and in cell growth medium for 7 days, the unseeded gels have a shear modulus of 0.06 kPa (not shown). A similar assay performed at the time of the initial characterization of the vim$^{-/-}$ mouse indicated that vimentin loss reduces fibroblast contractility (31), and using the culture densities (25 and 50 cells/μl) and gel material of the earlier study, we too find that vim$^{-/-}$ cells are less contractile than normal mEF (Fig. 6 *A*). However, this effect is cell-density and gel-composition dependent. Increasing cell density abrogates and eventually reverses the result such that vim$^{-/-}$ mEFs are more contractile than normal mEFs at $\geq$350 cells/μl (Fig. 6, *B–D*). It should be noted that mEFs are relatively similarly contractile across all conditions, whereas the contractility of the vim$^{-/-}$ mEF increases with seeding density. To control for possible differences in cell survival or proliferation, after 7 days in culture 3D constructs were fixed, stained with Hoechst, and cells counted. No significant differences between the normal and vim$^{-/-}$ mEFs were found at seeding densities up to 350 cells/μl; at 700 cells/μl nuclei are too closely spaced to distinguish individual cells (not shown). Nor did we note any obvious differences in the shapes (elongated) or distribution (homogeneous throughout the gel) of the two cell types. To verify that gels do not spontaneously change shape over time, unseeded gels were maintained alongside cell-seeded gels and handled in the same manner; no change in the appearance or diameter of the unseeded gels was observed (not shown).

To test whether gel composition could be mediating a signaling-based contractility difference, we substituted Fn for 5% of the collagen in the gel. Cultured in collagen + Fn gels, mEF, and vim$^{-/-}$ mEF contract more rapidly than in collagen without Fn, but they are equivalently contractile at all densities tested (175, 350, and 700 cell/μl),

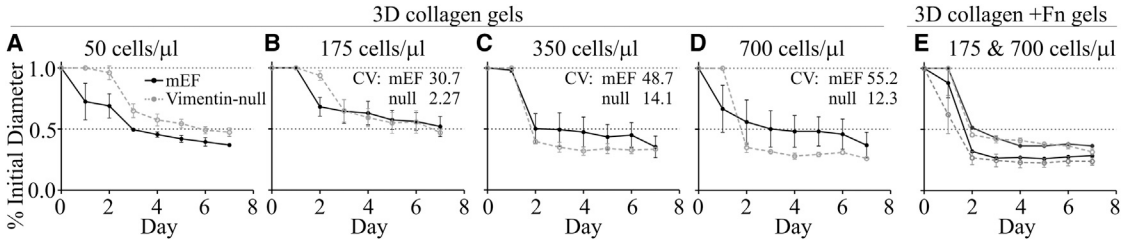

FIGURE 6 Contractility of vim$^{-/-}$ cells varies with cell density and gel composition. Normal or vim$^{-/-}$ mEFs were cultured in 2 mg/ml collagen gels for 7 days at densities of 25, 50 (*A*), 175 (*B*), 350 (*C*), or 700 (*D*) cells/μl. Gels were freed from the dish edge 24 h after plating, although some detached spontaneously and this underlies the differences evident on day 1. Seeded at 25 or 50 cells/μl, normal mEFs contract gels more than vim$^{-/-}$ mEFs (*A*). At 175 cells/μl, vim$^{-/-}$ mEFs are initially slower to contract but by 72 h after plating contract gels to the same extent as normal mEFs (*B*). Seeded at 350 or 700 cells/μl (*C* and *D*), vim$^{-/-}$ mEFs are more strongly contractile than normal mEFs in collagen gels. Seeding cells in gels composed of 95% collagen + 5% fibronectin increases the contractility of both cell types and equalizes their contractility (*E*). CV are average CV, days (3–7). All experiments performed $\geq$4 times; 1–3 replicates per condition per experiment.

and increasingly contractile with increasing cell number (Fig. 6 *E*). This result shows that the changes in contractility caused by vimentin loss are not purely reflective of an altered mechanical state.

DISCUSSION

The viscoelastic properties of gels formed by purified vimentin and other intermediate filament proteins are very different from those of other cytoskeletal networks, especially at large deformations. The large degree of strain stiffening and vimentin's unique ability to resist damage at strains >100% observed in vitro (9) suggest that vimentin is a primary determinant of cell mechanical properties, especially at large strains, and is therefore involved in the preservation of those properties in cells under stress. To test this hypothesis, we determined the effect of vimentin loss on the cells' viscoelastic properties.

Vimentin's contribution to cell elastic behavior is more subtle than might be expected for an abundant cytoskeletal protein, especially under minimally perturbing conditions. In part, this can be attributed to vimentin's much lower stiffness than F-actin, the low elastic modulus of vimentin gels at small deformations, and the scarcity of vimentin at the outermost cortical actin shell of mesenchymal cells. Vimentin network organization is consistent with a mechanical role that increases with the severity of a deformation. The characteristic IF network encircles the nucleus with densely packed filaments that radiate to the cell periphery with decreasing density (32). This organization implies that small inwardly directed strains, such as those produced by indentation of the cortex by an AFM cantilever, would meet mostly actin networks interspersed by relatively few compliant vimentin filaments. Deeper intrusions would encounter increasing numbers of strain-stiffening filaments. During AFM indentation experiments, the probe tip descends through the relatively stiff actin cortical layer of each cell (33–35), and although differences in internal elastic moduli between many cell types have been detected by AFM (e.g. (51)), it seems likely given the magnitude of the change caused by vimentin loss as detected by microrheology (10) that the small increase in elastic modulus attributable to vimentin could be obscured by the dominance of the relatively stiff actin cortex (36). In contrast, active microrheological measurements are less influenced by the mechanical properties of regions further from the oscillating bead (i.e., the cortex, in the case of an embedded bead) and more likely to detect small differences in internal properties (37).

These factors suggest that integrating the soft, elastic rheology of vimentin networks with the rapidly changeable mechanics of a stiffer, contractile actomyosin network maintains a more robust cellular mechanical response over a wide range of stress and strain levels than that which actomyosin can adopt by itself. We speculate that this, together with the extent of vimentin cross talk with other systems, helps to anchor or tune cell mechanical properties by integrating the inputs of other cytoskeletal, adhesion-related and additional systems. It seems likely that most experimental conditions are permissive for sufficient tension generation by actomyosin machinery, so that the latter system predominates (Fig. 7), although these results highlight the need to better understand the functions in vivo of the different cell viscoelastic properties. They also highlight the difficulty in distinguishing between the contributions of the actomyosin and vimentin networks. The two systems interact directly in vitro (38); are subject to coregulation (39,40), and a role for actin has recently been shown to regulate even microtubule-based vimentin transport (41). The lack of an IF-specific chemical disruptor compounds this difficulty by only allowing the interrelationship to be examined unidirectionally. Two vimentin-disrupting agents, withaferin A (42) and acrylamide (43,44), also affect microfilament organization. Furthermore, cell types on which many studies of actomyosin-based mechanical properties have been conducted also contain IF systems (e.g. (33,52)), and although the latter are often beyond the scope of such studies, the extent to which actin-directed perturbations also disrupt IF-mediated mechanical contributions is far from clear. No difference in actin expression levels or distribution have been reported for vim$^{-/-}$ mEF

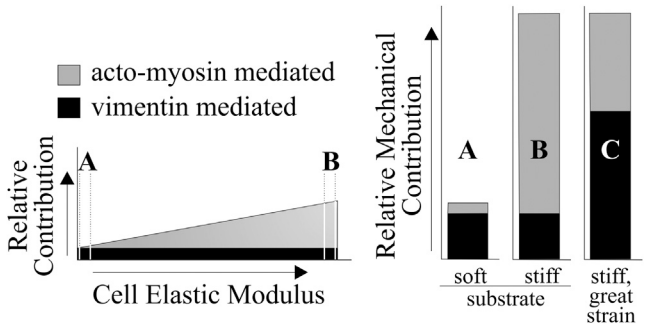

FIGURE 7 Model: Vimentin's mechanical role is enhanced in cells on soft substrates and by strain. Vimentin's mechanical characteristics may be more consistent (*black*) than those of the actomyosin system (*gray*) over a range of mechanical conditions. When actomyosin contractility is minimal, as in single cells on soft substrates (*A*), vimentin's mechanical properties could influence cell mechanical properties more than in cells in close proximity or on stiffer substrates (*B*). Vimentin's strain-stiffening properties are evident under conditions of large or unusual strain, particularly on hard substrates (*C*).

(e.g. (10,53)), but it is possible that more subtle changes in actin isoform expression, network distribution, or other signaling pathways are present, and that this loss of regulation could contribute to the variability in the spreading, stiffness, and PI of the vim$^{-/-}$ mEF.

We did not detect differences in the Young's moduli of the less spread cells. However, the same data show increased hysteresis in the forces measured by the descending and ascending strokes, particularly of the vim$^{-/-}$ mEF (Fig. 3). Thus, vimentin enhances cell elastic behavior, whereas its loss enhances cell fluidity (27). Because the loss-of-contact point in AFM studies was never more distal than the contact point, nor did the retraction curve ever dip to a lower force than the extension curve, and because there were no observable changes in the hysteresis over time to suggest the accrual or loss of adhesion with subsequent measurements, we conclude that cell-bead adhesion did not contribute to this effect. This enhancement of cell viscous behavior may help to explain the similarity between the Young's moduli of the two cell types on 6 kPa PAA. Although our model predicts that vimentin's mechanical contribution is greatest when cells are softest, this effect could be mitigated by the more fluid-like behavior under the same condition. It is possible, however, that when cells are not restricted to two-dimensional sparse growth conditions, vimentin's effect on cell mechanics could be evident despite the more viscous behavior, perhaps in a cell more completely tethered to neighboring structures or more extended in length. Our selection of similarly shaped cells or cells spread to similar areas may also have influenced this result, but unlike cells on traditional substrates, single cells grown under our experimental conditions offer less variability in these parameters.

After subculturing onto very soft substrates (~100 Pa), mEF and other cell types adhere and adopt persistently relatively spherical shapes (22,45). This failure to flatten and spread has been attributed to insufficient internal tension generation that is at least in part attributable to actomyosin systems (46,47,21). On slightly stiffer substrates with elastic moduli in the physiological range (>200 Pa) many cell types adopt greater spread areas, and spread area tends to increase with increasing substrate stiffness (22,24). More fluid behavior by the vim$^{-/-}$ mEF also explains these cells' greater spread areas on the hard substrate and their rapid initial spreading relative to normal mEF (Fig. 1 *G*). The jump in spread area that occurs after 26 min could be caused by a transition from an initial attachment mode characterized by contact formation, in which vimentin is less involved, to a subsequent spreading mode in which viscoelastic properties are more relevant, a conclusion supported by the timing of the transition (49) as well as recent work showing reduced cytoskeletal tension in vimentin-null fibroblasts attributable to the absence of vimentin's association with focal adhesions (50). Previous studies have also shown that vimentin remodeling precedes cell migration through small spaces (13), and that local remodeling occurs before lamellipodium formation (30), events that could be explained by vimentin's inhibition of the viscous flow of cytoplasm, which would necessitate network remodeling away from the cell periphery to facilitate cell shape change and membrane ruffling. The performance of prior studies on very stiff traditional substrates—on which fibroblasts are the least endogenously fluid and most altered by vimentin loss—further supports this possibility.

Finally, to assess vimentin's contribution to the cells' tension-generating ability, mEF and vim$^{-/-}$ mEF were cultured in 3D collagen gels. At low cell density, as shown previously, normal mEFs are more contractile than vim$^{-/-}$ mEFs (Fig. 6). However, when seeded more densely the normal and vim$^{-/-}$ mEFs contract the gels equally, and at greater seeding densities the vim$^{-/-}$ cells are more contractile than the normal mEFs. This result shows that vim$^{-/-}$ mEFs are capable of contracting as strongly as normal mEFs (Fig. 6 *E*). In collagen + Fn gels, however, both cell types are more strongly contractile than in collagen alone; and it is the normal mEFs that show the greatest change. Consistent with our model, vimentin enhances the tension-generating ability of minimally contacting cells in a very soft environment. As cell-cell interactions increase with cell density, actomyosin networks may increasingly pull against one another, rather than each straining against only the soft gel. In the highest-density seedings in which the vim$^{-/-}$ cells contract collagen gels more than the normal mEFs, it is possible that the strain-stiffening vimentin resists actin's tension-generating ability, and thus inhibits contractility.

CONCLUSION

Vimentin alters the relationship of the viscous and elastic components of cell elastic modulus. mEFs lacking vimentin

are more fluid, evidenced by their dissipation of a greater proportion of the energy needed to compress them than normal mEFs that behave more elastically after exposure to the same stress. Vimentin's enhancement of cell elastic behavior is more pronounced when cells are grown on a hard, rather than a soft, substrate. We also show a role for vimentin in the rate of cell spreading and the increase in cell elastic modulus attributable to increased spreading, previously recognized only as an actomyosin-mediated process. In addition to a contribution to the magnitude of cell viscoelastic properties, vimentin loss renders mEF significantly more variable in stiffness and plasticity than normal mEF, indicating that vimentin is an important regulator of these properties. Finally, vimentin's effect on the cells' contractile ability in 3D gels is cell-density and gel-composition dependent. $Vim^{-/-}$ mEFs seeded in collagen gels at low density are less contractile than normal mEFs, but more contractile at greater densities. Fn increases and equalizes the contractility of the two cell types. These results show that vimentin helps regulate cell viscoelastic properties in settings where cells are subjected to mechanical stresses at the timescales and force levels likely to occur in vivo.

This work was supported by the U.S. Public Health Service through grants National Institutes of Health-National Institute of General Medical Sciences (NIH-NIGMS) (PO1 GM096971) and National Heart, Lung, and Blood Institute (NHLBI) T32HL007954.

REFERENCES

1. Thiery, J. P., H. Acloque, …, M. A. Nieto. 2009. Epithelial-mesenchymal transitions in development and disease. *Cell.* 139:871–890.
2. Jiang, S. X., J. Slinn, …, S. T. Hou. 2012. Vimentin participates in microglia activation and neurotoxicity in cerebral ischemia. *J. Neurochem.* 122:764–774.
3. Satelli, A., and S. Li. 2011. Vimentin in cancer and its potential as a molecular target for cancer therapy. *Cell. Mol. Life Sci.* 68:3033–3046.
4. Farge, E. 2003. Mechanical induction of Twist in the *Drosophila* foregut/stomodeal primordium. *Curr. Biol.* 13:1365–1377.
5. Conway, D. E., M. T. Breckenridge, …, M. A. Schwartz. 2013. Fluid shear stress on endothelial cells modulates mechanical tension across VE-cadherin and PECAM-1. *Curr. Biol.* 23:1024–1030.
6. Ramsingh, R., A. Grygorczyk, …, R. Grygorczyk. 2011. Cell deformation at the air-liquid interface induces Ca2+-dependent ATP release from lung epithelial cells. *Am. J. Physiol. Lung Cell. Mol. Physiol.* 300:L587–L595.
7. Wang, H., S. M. Haeger, …, K. S. Anseth. 2012. Redirecting valvular myofibroblasts into dormant fibroblasts through light-mediated reduction in substrate modulus. *PLoS ONE.* 7:e39969.
8. Wells, R. G. 2013. Tissue mechanics and fibrosis. *Biochim. Biophys. Acta.* 1832:884–890.
9. Janmey, P. A., U. Euteneuer, …, M. Schliwa. 1991. Viscoelastic properties of vimentin compared with other filamentous biopolymer networks. *J. Cell Biol.* 113:155–160.
10. Guo, M., A. J. Ehrlicher, …, D. A. Weitz. 2013. The role of vimentin intermediate filaments in cortical and cytoplasmic mechanics. *Biophys. J.* 105:1562–1568.
11. Wang, N., and D. Stamenović. 2000. Contribution of intermediate filaments to cell stiffness, stiffening, and growth. *Am. J. Physiol. Cell Physiol.* 279:C188–C194.
12. Haudenschild, D. R., J. Chen, …, D. D. D'Lima. 2011. Vimentin contributes to changes in chondrocyte stiffness in osteoarthritis. *J. Orthop. Res.* 29:20–25.
13. Brown, M. J., J. A. Hallam, …, S. Shaw. 2001. Rigidity of circulating lymphocytes is primarily conferred by vimentin intermediate filaments. *J. Immunol.* 166:6640–6646.
14. Ofek, G., D. C. Wiltz, and K. A. Athanasiou. 2009. Contribution of the cytoskeleton to the compressive properties and recovery behavior of single cells. *Biophys. J.* 97:1873–1882.
15. Bertaud, J., Z. Qin, and M. J. Buehler. 2010. Intermediate filament-deficient cells are mechanically softer at large deformation: a multi-scale simulation study. *Acta Biomater.* 6:2457–2466.
16. Lulevich, V., H. Y. Yang, …, G. Y. Liu. 2010. Single cell mechanics of keratinocyte cells. *Ultramicroscopy.* 110:1435–1442.
17. Seltmann, K., A. W. Fritsch, …, T. M. Magin. 2013. Keratins significantly contribute to cell stiffness and impact invasive behavior. *Proc. Natl. Acad. Sci. USA.* 110:18507–18512.
18. Plodinec, M., M. Loparic, …, C. A. Schoenenberger. 2011. The nanomechanical properties of rat fibroblasts are modulated by interfering with the vimentin intermediate filament system. *J. Struct. Biol.* 174:476–484.
19. Kaufmann, A., F. Heinemann, …, R. Stick. 2011. Amphibian oocyte nuclei expressing lamin A with the progeria mutation E145K exhibit an increased elastic modulus. *Nucleus.* 2:310–319.
20. Lammerding, J., P. C. Schulze, …, R. T. Lee. 2004. Lamin A/C deficiency causes defective nuclear mechanics and mechanotransduction. *J. Clin. Invest.* 113:370–378.
21. Yeung, T., P. C. Georges, …, P. A. Janmey. 2005. Effects of substrate stiffness on cell morphology, cytoskeletal structure, and adhesion. *Cell Motil. Cytoskeleton.* 60:24–34.
22. Engler, A., L. Bacakova, …, D. Discher. 2004. Substrate compliance versus ligand density in cell on gel responses. *Biophys. J.* 86:617–628.
23. Sader, J. E., I. Larson, …, L. R. White. 1995. Method for the calibration of atomic-force microscope cantilevers. *Rev. Sci. Instrum.* 66:3789–3798.
24. Byfield, F. J., Q. Wen, …, P. A. Janmey. 2009. Absence of filamin A prevents cells from responding to stiffness gradients on gels coated with collagen but not fibronectin. *Biophys. J.* 96:5095–5102.
25. Li, Q. S., G. Y. Lee, …, C. T. Lim. 2008. AFM indentation study of breast cancer cells. *Biochem. Biophys. Res. Commun.* 374:609–613.
26. Costa, K. D. 2003-2004. Single-cell elastography: probing for disease with the atomic force microscope. *Dis. Markers.* 19:139–154.
27. Klymenko, O., J. Wiltowska-Zuber, …, W. M. Kwiatek. 2009. Energy dissipation in the AFM elasticity measurements. *Acta Phys. Pol. A.* 115:548–551.
28. Solon, J., I. Levental, …, P. A. Janmey. 2007. Fibroblast adaptation and stiffness matching to soft elastic substrates. *Biophys. J.* 93:4453–4461.
29. Lynch, C. D., A. M. Lazar, …, M. P. Sheetz. 2013. Endoplasmic spreading requires coalescence of vimentin intermediate filaments at force-bearing adhesions. *Mol. Biol. Cell.* 24:21–30.
30. Helfand, B. T., M. G. Mendez, …, R. D. Goldman. 2011. Vimentin organization modulates the formation of lamellipodia. *Mol. Biol. Cell.* 22:1274–1289.
31. Eckes, B., D. Dogic, …, T. Krieg. 1998. Impaired mechanical stability, migration and contractile capacity in vimentin-deficient fibroblasts. *J. Cell Sci.* 111:1897–1907.
32. Sivaramakrishnan, S., J. V. DeGiulio, …, K. M. Ridge. 2008. Micromechanical properties of keratin intermediate filament networks. *Proc. Natl. Acad. Sci. USA.* 105:889–894.
33. Pourati, J., A. Maniotis, …, N. Wang. 1998. Is cytoskeletal tension a major determinant of cell deformability in adherent endothelial cells? *Am. J. Physiol.* 274:C1283–C1289.
34. Costa, K. D., A. J. Sim, and F. C. P. Yin. 2006. Non-Hertzian approach to analyzing mechanical properties of endothelial cells probed by atomic force microscopy. *J. Biomech. Eng.* 128:176–184.

35. Sato, M., D. P. Theret, …, R. M. Nerem. 1990. Application of the micropipette technique to the measurement of cultured porcine aortic endothelial cell viscoelastic properties. *J. Biomech. Eng.* 112:263–268.

36. Nawaz, S., P. Sánchez, …, I. A. T. Schaap. 2012. Cell visco-elasticity measured with AFM and optical trapping at sub-micrometer deformations. *PLoS ONE.* 7:e45297.

37. Hoffman, B. D., G. Massiera, …, J. C. Crocker. 2006. The consensus mechanics of cultured mammalian cells. *Proc. Natl. Acad. Sci. USA.* 103:10259–10264.

38. Esue, O., A. A. Carson, …, D. Wirtz. 2006. A direct interaction between actin and vimentin filaments mediated by the tail domain of vimentin. *J. Biol. Chem.* 281:30393–30399.

39. Tint, I. S., P. J. Hollenbeck, …, A. D. Bershadsky. 1991. Evidence that intermediate filament reorganization is induced by ATP-dependent contraction of the actomyosin cortex in permeabilized fibroblasts. *J. Cell Sci.* 98:375–384.

40. Hubert, T., J. Vandekerckhove, and J. Gettemans. 2011. Unconventional actin conformations localize on intermediate filaments in mitosis. *Biochem. Biophys. Res. Commun.* 406:101–106.

41. Robert, A., H. Herrmann, …, V. I. Gelfand. 2014. Microtubule-dependent transport of vimentin filament precursors is regulated by actin and by the concerted action of Rho- and p21-activated kinases. *FASEB J.*: (In press).

42. Grin, B., S. Mahammad, …, R. D. Goldman. 2012. Withaferin a alters intermediate filament organization, cell shape and behavior. *PLoS ONE.* 7:e39065.

43. Aggeler, J., and K. Seely. 1990. Cytoskeletal dynamics in rabbit synovial fibroblasts: I. Effects of acrylamide on intermediate filaments and microfilaments. *Cell Motil. Cytoskeleton.* 16:110–120.

44. Arocena, M. 2006. Effect of acrylamide on the cytoskeleton and apoptosis of bovine lens epithelial cells. *Cell Biol. Int.* 30:1007–1012.

45. Byfield, F. J., R. K. Reen, …, K. J. Gooch. 2009. Endothelial actin and cell stiffness is modulated by substrate stiffness in 2D and 3D. *J. Biomech.* 42:1114–1119.

46. Engler, A. J., M. A. Griffin, …, D. E. Discher. 2004. Myotubes differentiate optimally on substrates with tissue-like stiffness: pathological implications for soft or stiff microenvironments. *J. Cell Biol.* 166:877–887.

47. Kumar, S., I. Z. Maxwell, …, D. E. Ingber. 2006. Viscoelastic retraction of single living stress fibers and its impact on cell shape, cytoskeletal organization, and extracellular matrix mechanics. *Biophys. J.* 90:3762–3773.

48. Reference deleted in proof.

49. Greiner, A. M., H. Chen, …, R. Kemkemer. 2013. Cyclic tensile strain controls cell shape and directs actin stress fiber formation and focal adhesion alignment in spreading cells. *PLoS ONE.* 8:e77328.

50. Gregor, M., S. Osmanagic-Myers, …, G. Wiche. 2013. Mechanosensing through focal adhesion-anchored intermediate filaments. *FASEB J.* 28:715–729.

51. Pogoda, K., J. Jaczewska, …, M. Lekka. 2012. Depth-sensing analysis of cytoskeleton organization based on AFM data. *Eur. Biophys. J.* 41:79–87.

52. Kasas, S., X. Wang, …, S. Catsicas. 2005. Superficial and deep changes of cellular mechanical properties following cytoskeleton disassembly. *Cell Motil. Cytoskeleton.* 62:124–132.

53. Colucci-Guyon, E., M. M. Portier, …, C. Babinet. 1994. Mice lacking vimentin develop and reproduce without an obvious phenotype. *Cell.* 79:679–694.